Available online at www.sciencedirect.com
SCIENCE DIRECT®
International Journal of Mass Spectrometry 235 (2004) 229–241
International Journal of Mass Spectrometry
www.elsevier.com/locate/ijms

Cluster composition distribution at the liquid surface of alcohol–water mixtures and evaporation processes studied by liquid ionization mass spectrometry

Masahiko Tsuchiya [a,b,*], Yasuo Shida [b], Kenichi Kobayashi [c], Osamu Taniguchi [c], Shoichi Okouchi [c]

[a] *Yokohama National University, Hodogaya, Yokohama, Japan*
[b] *Tokyo University of Pharmacy and Life Science, Horinouchi, Hachiohji, Tokyo, Japan*
[c] *Department of Material Chemistry, Hosei University, Kajinomachi, Koganei, Tokyo, Japan*

Received 30 January 2004; accepted 22 March 2004

Abstract

Liquid ionization mass spectrometry (LPI-MS) gives information about hydrogen-bonded clusters at a liquid surface. By improving the way in which samples are introduced, mass spectra showing clusters at the liquid surface or in a gas phase were obtained for 20% (v/v) ethanol and methanol aqueous solutions. Observed cluster ions were expressed as $(ROH)_m(H_2O)_nH^+$, R = CH_3 or C_2H_5, and mass spectra gave the molar ratios of methanol to water (*M*/*W*) or ethanol to water (*E*/*W*) close to the ratio corresponding to the concentration of the respective solution. Binary cluster ions containing two molecules of alcohol ($m = 2$) were abundant for both solutions. The molar ratios calculated from the cluster compositions, $m - n$, of the most abundant cluster ions were also close to the ratio corresponding to the concentration of the solution. The results suggest that the composition distribution of cluster ions observed as LPI mass spectrum may be similar to the composition distribution of clusters existing at the liquid surface.

The cluster compositions at the liquid surface vary very quickly due to evaporation of the liquid. The clusters in the vapor were also measured using another device for sample introduction. The evaporation processes occurring in the nano-space at and above the liquid surface were mainly the loss of water molecules from larger clusters. The following collisions between smaller clusters leaded to the association of alcohol molecules accompanied with further loss of water molecules, resulting in the increase of the number of alcohol molecules in each cluster. Even ethanol clusters, $(C_2H_5OH)_mH^+$, were formed from the aqueous ethanol solutions. Reasonable differences between ethanol–water and methanol–water were observed for the mass spectra measured in the gas phase. Liquid ionization mass spectrometry gives nano-scale information concerning the cluster compositions at the liquid surface and the evaporation processes.

Keywords: Clusters at liquid surface; Methanol–water clusters; Ethanol–water clusters; Liquid ionization mass spectrometry; Evaporation processes

1. Introduction

Studies of clusters in gas and liquid phases under atmospheric pressure are very important for understanding the properties and structures of liquids and also for understanding chemical reactions in solutions. Many studies [1–6] have been reported concerning the association and dissociation mechanisms and the structures of clusters and cluster ions. The theoretical calculation for the structures of clusters has also been developed [7].

Mass spectrometry is a useful method for obtaining information about the distribution of cluster sizes (molecular composition). Clusters in gas and condensed phases have been investigated by mass spectrometry with several techniques [1–6,8,9]. The supersonic free jet expansions have been the most widely utilized methods for generating clusters. Neutral clusters or cluster ions are produced in vacuum by an expansion of a sample vapor mixed with inert gas at high pressure through a molecular beam nozzle [1–6]. Another method is the adiabatic expansion of a liquid jet,

* Corresponding author. Present address: 4-37-27 Kugayama, Suginami, Tokyo 168-0082, Japan

1387-3806/$ – see front matter © 2004 Elsevier B.V. All rights reserved.
doi:10.1016/j.ijms.2004.03.014

in which a sample liquid is directly fed to a vacuum system through an injector nozzle, and droplets explode adiabatically into a high vacuum [8,9]. Resulting clusters are ionized by electron ionization or photo-ionization. These methods are useful in obtaining information about the stabilities and the kinetics of association and dissociation concerning neutral clusters and/or cluster ions.

Utilizing a laser beam, isolated clusters or cluster ions have been studied by ultraviolet (UV) and infrared (IR) spectrometry. The clusters just above the liquid surface have been measured by this method [10]. Although the optical spectrometric methods are useful for interrogating the structure of isolated clusters, they do not provide information about the size distribution of clusters. In the previous methods involving mass spectrometric techniques, clusters have been produced in vacuum by adiabatic expansion (low temperature). Observed cluster ions for ethanol–water mixtures have been mostly pure ethanol cluster ions $(C_2H_5OH)_mH^+$, accompanied by small numbers of large binary cluster ions $(C_2H_5OH)_m(H_2O)_nH^+$ [9]. The molar ratios of ethanol to water calculated from observed mass spectra have been larger than expected when compared with those calculated from the ethanol concentrations of the sample solutions.

The cluster ion containing 21 molecules of water has been well known as the magic number cluster of water [1,2]. It has also been reported for alcohol–water mixtures that the intensity distributions of $(CH_3OH)_m(H_2O)_nH^+$ show magic numbers, $m + n = 21$, $0 < m < 8$, due to the enhanced stabilities of the dodecahedral cage structures in the mixed clusters [11]. It has been reported on the magic number clusters of mixtures that methanol molecules have substitutional interaction with water clusters, while acetonitrile molecules have additional interaction with water clusters [12]. As described in this paper, such magic number stabilities were also observed for both methanol–water and ethanol–water mixtures.

The surface compositions of ethanol–water mixtures have been measured by sampling the binary vapor in equilibrium with the mixture, with the aid of a time of flight mass spectrometer [13]. The surface mole fractions (X_E) obtained from their mass spectra have been higher than the X_E in the liquids and agreed with other methods, such as surface tension and neutron diffraction methods. The vapor–liquid equilibrium diagrams (isothermal) have been measured previously for various binary systems, indicating that the ethanol (and also methanol) concentration in vapor is higher than that in the liquid. The mole fraction of ethanol (X_E) in the vapor at 30 °C has been reported as 0.38 for 20% (v/v) ethanol aqueous solution ($X_E = 0.072$ in the liquid) [14].

1.1. Liquid ionization (LPI) mass spectrometry

We have developed a soft ionization method, termed liquid ionization mass spectrometry [15–17] (referred to as LPI since 1998 [17]), in which a liquid sample is ionized by collision with excited argon atoms (Ar*) under atmospheric pressure. The method (LPI-MS) has been applied to studies of clusters, such as water [18–20], carboxylic acid-water mixtures [17,21], and ethanol–water mixtures [22–25]. Recently, it has become clear that the method is appropriate to investigate hydrogen-bonded clusters, which exist at the surface of liquids and also in a gas phase under atmospheric pressure [17,18,24,25].

In the case of ethanol–water mixtures, abundant binary cluster ions have been observed by LPI-MS and the following reactions (reactions 1–3) have been assumed to occur [17,25].

$$\mathrm{Ar}^* + (C_2H_5OH)_a(H_2O)_b \rightarrow (C_2H_5OH)_a(H_2O)_b{}^+ + e^- + \mathrm{Ar} \quad (1)$$

$$\mathrm{Ar}^* + (C_2H_5OH)_a(H_2O)_b \rightarrow (C_2H_5OH)_c(H_2O)_dH^+ + (C_2H_5OH)_e(H_2O)_f(OH)^- + \mathrm{Ar}; \quad a, b > c, d \quad (2)$$

$$(C_2H_5OH)_c(H_2O)_dH^+ + (C_2H_5OH)_m(H_2O)_n \rightarrow (C_2H_5OH)_{m'}(H_2O)_{n'}H^+ + (C_2H_5OH)_{c'}(H_2O)_{d'}; \quad m, n > c, d; \quad m', n' > c,' d' \quad (3)$$

Although metastable Ar atoms (Ar*) ionize clusters at the liquid surface as shown by reaction 1, cluster ions observed were all protonated. Therefore, reaction 2 and proton transfer reactions like reaction 3 must follow to produce final cluster ions, $(C_2H_5OH)_{m'}(H_2O)_{n'}H^+$. It is very important to estimate how big the differences are between m, n, and m', n' in reaction 3.

We have reported previously that if a sample liquid was supplied directly to the needle tip (sample holder), the molar ratios of ethanol to water (E/W) calculated from LPI mass spectra became closer to the molar ratio calculated from its concentration of the solution [23–25]. In contrast, if the sample was vaporized near the needle tip, mass spectra showed abundant ethanol cluster ions [22,23], which looked similar to those observed by the adiabatic expansion method [9].

LPI mass spectral patterns are affected by several experimental conditions, such as the flow rate of Ar gas, the flow rates of a sample solution and the surface area of the liquid. Large cluster ions decrease in abundance with Ar flow rate and result in abundant smaller cluster ions containing smaller numbers (n) of water molecules [24]. The results indicate that evaporation occurs more rapidly with higher Ar flow rates. The flow rate of a sample solution should be controlled to obtain better results. The compositions of ethanol–water clusters must vary very quickly during the evaporation of clusters at the liquid surface. The parameters mentioned above affect the evaporation processes in nano-space at the liquid surface.

Van der Waals clusters can be observed by other methods, which utilize the adiabatic expansion in vacuum. In contrast,

those clusters have never been observed by LPI-MS. A variety of results obtained by LPI-MS indicate that all cluster ions are produced in the ion source and the adiabatic expansion does not occur in LPI-MS [17,25].

Good results have been obtained for 40% ethanol aqueous solution, but the results for 20% ethanol aqueous solution have been poor, which means that observed molar ratios (E/W) were much higher than the ratio calculated from the concentration of the solution [25]. Therefore, we improved the device for sample introduction and good results were obtained. This paper describes the distribution of cluster compositions ($m - n$) at the liquid surface, the evaporation phenomena and the structure of liquids.

2. Experimental

Several mass spectrometers, specially designed for LPI, have been used for cluster studies [17,18,20,24]. Recently, we have succeeded to modify a quadrupole mass spectrometer commercially available (Hitachi M1000 LC/MS, Japan) for measuring LPI mass spectra. A part of its ESI ion source was modified. The voltages for ion focusing were lowered and the interface was kept at ambient temperature [25]. A sample holder like device (A) (shown in Fig. 1) has been used. A Teflon block covered the needle and a liquid sample flew inside the block up to the needle tip [17,25]. Although good results have been obtained for 40% ethanol aqueous solution [25], it was still not easy to obtain good mass spectra for 20% (v/v) ethanol aqueous solutions.

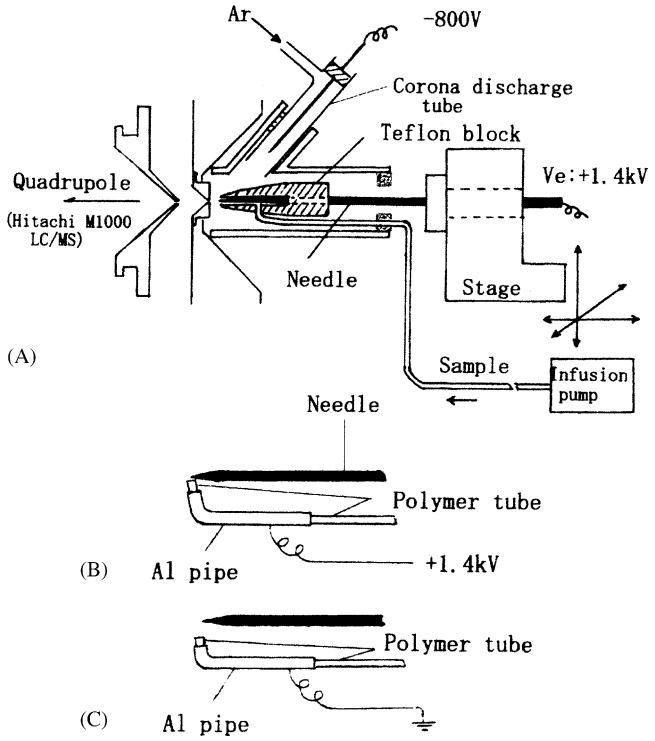

Fig. 1. Schematic diagram of liquid ionization (LPI) ion source with devices (A), (B) and (C) for introducing a sample. (A) or (B) is used for measuring clusters at liquid surface, while (C) is for measuring clusters in a gas phase.

When the end of a polymer tube for introducing a sample solution was placed close to the needle tip and the tube was covered with a metal (aluminum) pipe as shown in Fig. 1B (device B), good LPI mass spectra were obtained at an adequate flow rate of the solution. The inside diameter of the polymer tube (for HPLC) was 1 mm. The needle tip touched only slightly with the liquid surface at an appropriate flow rate of the solution. The flow rate was controlled using an infusion pump (Harvard Apparatus 22, USA). In addition, a high voltage was applied to the metal (aluminum) pipe in order to ionize all clusters at the liquid surface prior to evaporation. In this study, the metal pipe was connected to the needle (sample holder), which was kept at 1.4 kV.

Another device (C) (Fig. 1C) was used for measuring clusters in a gas phase in order to investigate the evaporation processes of clusters (neutral) on the liquid surface. Although the device (C) looks similar to the device (B), they differed in that the needle tip was placed 3 mm above the end of the polymer tube and the metal (Al) pipe was grounded. Because the recombination of positive ions and negative ions (or electrons) is very rapid under atmospheric pressure [17], cluster ions produced at the liquid surface were neutralized at the earth potential and only neutral clusters evaporated from the liquid surface were ionized at the needle tip, being observed as LPI mass spectra.

The flow rate of Ar with Ar* was kept at 500 ml/min, because higher flow rates promoted the dissociation of clusters due to evaporation [24] and lower flow rates made corona discharge unstable. The voltage applied to the needle (V_E) was 1.4 kV, because mass spectral patterns were almost the same at V_E of 1.3–1.5 kV, although the ion abundance increased with the voltage, but too high voltage caused a sort of arc discharge, resulting in abundant small cluster ions. The temperature of samples was ambient (ca. 25 °C). The open area of the ion source (opposite to the pinhole) was narrowed with the soft polymer plate (shown in Fig. 1) in order to obtain the maximum ion abundance.

Mass spectra were obtained by scanning the mass range from m/z 10 to 600 in 2 s or to 1000 in 3 s, and by recording repeatedly for 50–100 mass spectra. Each mass spectrum shown here is the average of 50 mass spectra recorded in succession. The experimental parameters in the detection system related to the ion abundance were maintained as constant as possible. Other experimental conditions were the same as those reported previously [17,25]. If the pinhole (diameter: 200 μm) became dirty with any contamination, large cluster ions decomposed due to the space charge on the contamination and only small cluster ions were observed. Therefore, the pinhole and skimmers were kept clean.

2.1. Samples

Ethanol–water and methanol–water binary mixtures (20% v/v aqueous solutions) were prepared by mixing ethanol (or

methanol) and pure water, all commercially available for HPLC (Wako, Osaka, Japan).

3. Results and discussion

3.1. 20% (v/v) ethanol aqueous solution

3.1.1. Cluster composition distribution at the liquid surface measured using the devices (A) and (B)

All cluster ions observed in the LPI mass spectra were represented as $(C_2H_5OH)_m(H_2O)_nH^+$ (referred to as $m - n$). As previously reported, LPI mass spectra of 20% ethanol solution measured using the device (A) (Fig. 1A) have given much higher molar ratios of ethanol to water ($E/W = 0.23$–0.28) than the ratio corresponding to the concentration of the solution ($E/W = 0.078$) [24,25]. Although better results were obtained by controlling the sample flow rate, the E/W ratios (0.11–0.17) calculated from those mass spectra were still higher than the ratio of the concentration.

In order to ionize the liquid surface closest to the bulk, a new device (B) (Fig. 1B) was examined and better results were obtained with B at the appropriate flow rates of the sample solution. The mass spectra shown in Fig. 2a gave the lowest molar ratio of ethanol to water ($E/W = 0.082$ as shown in Table 1) so far obtained. The ratio is close to that of the concentration of the solution. The base peak appearing at $m/z = 561$ corresponds to the cluster ions with $m - n = 2$–26 (indicated on Fig. 2a).

3.1.2. Digital expression of a mass spectrum

Table 1 is a digital expression of the mass spectrum shown in Fig. 2a. The numbers in the top column (E0–E6) mean the number of ethanol molecules ($m = 0$–6) in each cluster ion and the numbers in the left end column (n) mean the number of water molecules in each cluster ion. All figures inside Table 1 (and other tables, too) present the peak intensities corresponding to the abundance of cluster ions with the same composition, $m - n$. E2 means the cluster ions containing two molecules of ethanol ($m = 2$, $n = 0$–n), E0 ($m = 0$) means cluster ions of water, $(H_2O)_nH^+$, and $n = 0$ means cluster ions of ethanol, $(C_2H_5OH)_mH^+$. It should be noted that no ethanol cluster ions ($n = 0$) were observed at the liquid surface.

The cross sections of Penning ionization (reaction 1) and of proton transfer reactions (reactions 2 and 3) are not known. The ionization energies of molecular water, water dimer and ice have been reported as 12.2, 11.5 and 11.2 eV, respectively [26], suggesting that the cross sections of ionization and of proton transfer reactions for these clusters

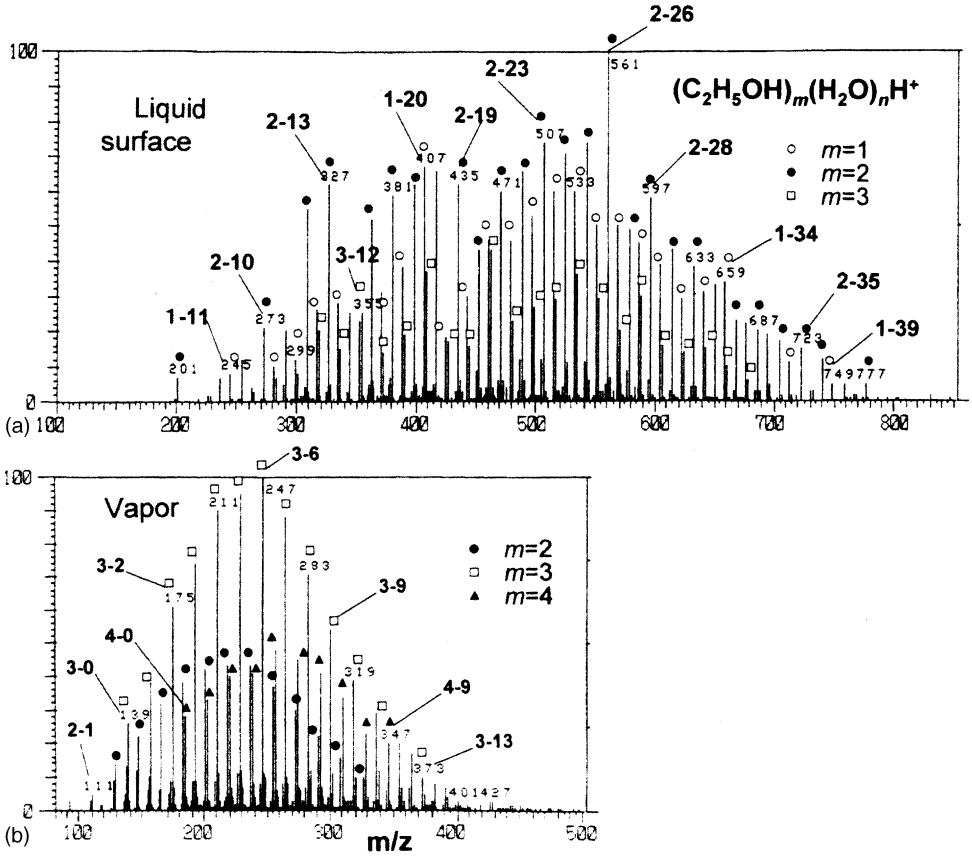

Fig. 2. LPI mass spectra of 20% (v/v) ethanol aqueous solution: (a) measured at the liquid surface using the device B (sample flow rate: 0.8 μl/min) and (b) measured in the gas phase using the device C (sample flow rate: 0.3 μl/min).

Table 1
Digital expression of LPI mass spectrum (Fig. 2a) of 20% ethanol solution measured with device B; peak intensity > 640 = R.I. > 1.5%, > 210 = R.I. > 0.5%, R.I.: relative ion abundance = $Im - n$/total ions

$n \backslash m$	E0	E1	E2	E3	E4	E5	E6	ΣIn	$n\Sigma In$
0									
1									
2									
3									
4									
5									
6			103					103	**618**
7				51				51	**357**
8			113	112	81			306	**2448**
9			182	125			44	351	**3159**
10			311	291	63	49		714	**7140**
11		118	299	223				640	**7040**
12		68	797	370	76			1311	**15732**
13		150	890	211		59		1310	**17030**
14		181	357	274	98			910	**12740**
15		380	745	527	59			1711	**25665**
16	73	403	843	252	93	44		1708	**27328**
17	58	331	887	230	97			1603	**27251**
18	43	454	940	624	56	54		2171	**39078**
19	55	551	889	331	164			1990	**37810**
20	84	965	625	398	95			2167	**43340**
21	104	269	857	426	101			1757	**36897**
22	48	430	949	522				1949	**42878**
23	75	662	1067	423				2227	**51221**
24	55	665	1015	296				2031	**48744**
25	132	766	1056	428	58			2440	**61000**
26	99	856	1424	240				2619	**68094**
27	179	864	703	203				1949	**52623**
28	181	715	829	220	55			2000	**56000**
29	58	713	616	148				1535	**44515**
30	163	653	551	96				1463	**43890**
31	78	560	473	77				1188	**36828**
32	140	427	336					903	**28896**
33	90	455	294	47				886	**29238**
34	54	487	249					790	**26860**
35	65	325	215					605	**21175**
36		279	175					454	**16344**
37	54	166	78					298	**11026**
38	46	52	83					181	**6878**
39		79						79	**3081**
ΣIm	1934	13024	18951	7145	1096	206	44	42400	
$m\Sigma Im$		**13024**	**37902**	**21435**	**4384**	**1030**	**264**		**952924**
							78039	***E/W*=0.082**	

may be similar to each other. Because no calibration standard was available, the peak intensities of all ions recorded by the data system (Hitachi M1000) were simply presented in the tables. Table 1 presents not only the peak intensities, but also the composition ($m - n$) distribution of observed cluster ions and the calculated molar ratio E/W.

3.1.3. Molar ratio of ethanol to water (E/W)

The sum of peak intensities of cluster ions containing m molecules of ethanol is shown in the bottom of Table 1, as $\sum Im$ (I: peak intensity). The sum ($\sum Im$) multiplied by the number m, which is $m\sum Im$ as shown in the bottom of Table 1, is assumed to be proportional to the total number of ethanol molecules in the cluster ions containing m molecules of ethanol. The sum (E) of $m\sum Im$ ($m = 0$–6) calculated from the whole mass spectrum is also assumed to be proportional to the total number of ethanol molecules in all cluster ions.

In the same way, the sum (W) of $n\sum In$ ($n = 0$–39 in Table 1) calculated from the whole mass spectrum can be assumed to be proportional to the total number of water molecules in all ions. Thus, the molar ratio (E/W) calculated from the spectrum shown in Table 1 (=Fig. 2a) is 0.082 (78039/952924).

Although 0.082 is still slightly higher than the ratio of the concentration, the base peak appearing at $m/z = 561$ corresponds to the cluster ions of 2–26 ($m - n$) and the molar ratio calculated from the base peak composition ($m/n = 2/26$) is 0.077, which coincides the concentration of the solution. In addition, it is interesting to note that the cluster ions around the base peak, which have the molecular compositions similar to the concentration, are abundant.

Table 2
Digital expression of LPI mass spectrum of the 20% ethanol solution measured with device B; peak intensity > 770 = R.I. > 1.5%, > 260 = R.I. > 0.5%

n \ *m*	E0	E1	E2	E3	E4	E5	E6	Σ*In*	*n*Σ*In*
0									
1									
2									
3									
4									
5							71	71	**355**
6			145					145	**870**
7			144	121	68			333	**2331**
8			**386**	68				454	**3632**
9		106	**501**	105			72	784	**7056**
10		178	**399**	90				667	**6670**
11		**318**	**642**	179	112			1251	**13761**
12		**590**	1009	241	127	106		2073	**24876**
13	110	**527**	1118	244		86		2085	**27105**
14		**719**	1267	**329**	148	89		2552	**35728**
15	83	789	1105	**383**	69			2429	**36435**
16	144	744	1411	**349**	94		66	2808	**44928**
17	167	1085	1562	**296**				3110	**52870**
18	190	1173	1722	**465**	90			3640	**65520**
19	218	1209	**2130**	324				3881	**73739**
20	204	**1548**	1179	257				3188	**63760**
21	**276**	935	1355	390				2956	**62076**
22	174	1007	1250	322				2753	**60566**
23	**280**	1083	1146	188				2697	**62031**
24	226	1161	1047	140				2574	**61776**
25	**282**	1233	838	243				2596	**64900**
26	165	904	**744**	89				1902	**49452**
27	223	880	577	110				1790	**48330**
28	132	**469**	**336**	81				1018	**28504**
29	89	**584**	**287**					960	**27840**
30	153	**308**	**316**	70				847	**25410**
31	101	**275**	187					563	**17453**
32	82	183	130					395	**12640**
33		116	72					188	**6204**
34		92	92					184	**6256**
35		95						95	**3325**
Σ*Im*	3299	18311	23097	5084	708	281	209	50989	
m*Σ*Im		**18311**	**46194**	**15252**	**2832**	**1405**	**1254**		**996399**
							85248	***E/W*=0.086**	

Another mass spectrum measured at the sample flow rate of 0.9 μl/min using the new device (B) is shown in Table 2. Although the ratio (0.086) is slightly higher than that in Table 1, most abundant cluster ions are those containing two molecules of ethanol ($m = 2$), as same in both Tables. The base peak (*m/z* 435) corresponds to the cluster ions of 2–19, which were often observed for 20% ethanol solutions.

In general, ethanol solutions are thought to be uniform from the micro-scale point of view. The concentration (0.078) indicates that an average number of water molecules (n) should be 13 in the case of $m = 1$, 26 in the case of $m = 2$ and 39 in the case of $m = 3$. In addition, the compositions of abundant cluster ions shown in Tables 1 and 2 have the molar ratios (m/n) similar to that of the concentration. It should be noted that the ethanol cluster ions, $(C_2H_5OH)_mH^+$, and also binary cluster ions with $n = 1$–4 are not observed in Tables 1 and 2. In contrast, those cluster ions have been observed abundantly by other methods using the adiabatic expansion.

3.1.4. Clusters in the gas phase near the liquid surface

LPI mass spectra obtained with the device (A) have often presented the cluster ions containing three molecules of ethanol as the most abundant ions. The increase in the number of ethanol molecules, from 2 to 3, has been considered as the results of evaporation [24]. Therefore, LPI mass spectra were measured using the device (C) (Fig. 1C). Clusters evaporated from the liquid at the end of the polymer tube were ionized at the needle tip 3 mm above the liquid surface. An example shown in Fig. 2b and Table 3 (digital expression of Fig. 2b) presents the composition distribution of clusters in the gas phase (vapor), that is, abundant smaller cluster ions compared with those shown in Fig. 2a and Tables 1 and 2.

Table 3 clearly indicates that the numbers of water molecules in cluster ions decreased significantly (from 8–38 to 0–16) and even pure ethanol cluster ions, $(C_2H_5OH)_mH^+$, $m = 2$–6, appeared. In contrast, the numbers of ethanol molecules in abundant cluster ions increased from 1–3 to 2–5.

Table 3
Digital expression of the mass spectrum (Fig. 2b) of 20% ethanol solution measured with device C; peak intensity > 1480 = R.I. > 1.5%, > 490 = R.I. > 0.5%

$n \setminus m$	E 0	E 1	E 2	E 3	E 4	E 5	E 6	E7	ΣIn	$n\Sigma In$
0			172	**1472**	1579	432	370		4025	
1			288	2094	1828	**567**	239		5016	**5016**
2			**801**	3382	2222	468	165	183	7221	**14442**
3			**1242**	4075	2270	**692**	265		8544	**25632**
4			1805	4968	2672	**632**			10077	**40308**
5		314	2121	5268	2522	**600**			10825	**54125**
6		332	2321	**5500**	2269	**711**			11133	**66798**
7		**513**	2391	4888	1910	404			10106	**70742**
8		**536**	2413	3933	**1284**	279			8445	**67560**
9		**510**	2039	2983	**1147**	239			6918	**62262**
10		**642**	1652	2178	**963**				5435	**54350**
11		483	**1213**	1605	445	173			3919	**43109**
12	185	467	**916**	**1123**	179				2870	**34440**
13		429	**560**	**572**					1561	**20293**
14	211	232	354	414					1211	**16954**
15	166	173	402						741	**11115**
16		190	207	178					575	**9200**
ΣIm	562	4821	20897	44633	21290	5197	1039	183	98622	
$m\Sigma Im$		**4821**	**41794**	**133899**	**85160**	**25985**	**6234**	**1281**		**596346**
								299174	*E/W*=0.502	

It is certain that these prominent changes in the cluster compositions occur during evaporation at and above the liquid surface, because no ions can evaporate from the liquid and get through the pinhole in the LPI ion source. Only neutral clusters are ionized at the needle tip to be observed as LPI mass spectrum [17]. It is very interesting to note that ethanol cluster ions, $(C_2H_5OH)mH^+$, were observed in the gas phase.

As a result, the *E*/*W* ratio increased to 0.50. It is also interesting to note that the base peak (*m*/*z* 247) corresponding to the cluster ions (3–6) gives the molar ratio ($m/n = 0.50$) equal to the averaged *E*/*W* ratio (0.50) as shown in Table 3. The increase of the *E*/*W* ratios in vapor phase is reasonable, because the mole fraction of ethanol (X_E) in the vapor of 20% ethanol solution has been reported as 0.38 (*E*/*W* = 0.61) [14].

3.2. 20% (v/v) methanol aqueous solution

3.2.1. Cluster composition distribution at the liquid surface

An example of a mass spectrum obtained from a 20% (v/v) methanol aqueous solution measured with the device B is shown in Fig. 3a and Table 4 (digital expression of Fig. 3a). The cluster ions containing two alcohol molecules are also abundant in the methanol solution, although the molar ratio ($M/W = 0.111$) is slightly higher than the ratio ($E/W = 0.078$) of the ethanol solution. Therefore, cluster ions containing four molecules of methanol are observed in Fig. 3a. The distribution of cluster compositions can be seen more clearly in Table 4, which indicates that the molar ratio of methanol to water ($M/W = 0.112$) calculated from the mass spectrum agreed well with the *M*/*W* ratio (0.111) corresponding to the concentration of the solution. The base peak shown in Fig. 3a appearing at $m/z = 407$ corresponds to the cluster ions of 2–19. The molar ratio corresponding to the base peak ($m/n = 2/19$) is 0.105 and the abundant cluster ions are observed around the base peak, showing one round distribution of the peak intensities. Therefore, the averaged molar ratio (*M*/*W*) agreed with the ratio of the concentration. Judging from the results of many experiments, it seems easier to obtain LPI mass spectra giving the molar ratios close to the concentration for methanol–water mixtures, compared with the ratios for ethanol–water mixtures.

3.2.2. Clusters in the gas phase

Examples of mass spectra of the 20% methanol solution measured with the device C are shown in Fig. 3b, Table 5 (digital expression of Fig. 3b) and Table 6. These figure and tables indicate that the number of methanol molecules in cluster ions clearly increased, while the number of water molecules decreased during evaporation. These tendencies were similar to those observed for the ethanol solution. The increase in the number of methanol molecules, however, is observed more significantly, especially for Table 6 ($m = 1$–$4 \rightarrow 3$–8), compared with the case for the ethanol solution. In contrast, the decrease in the number of water molecules is less significant. Only a few methanol cluster ions were observed even in the gas phase (Table 5). Table 5 was measured with the sample flow rate of 0.8 μl/min and Table 6 was measured with 0.3 μl/min. In the latter, the further evaporation may be expected to occur.

The cluster ions, 1–18 to 1–33, shown in Table 6 have the same mass numbers as those of 10–2 to 10–17. Therefore, the latter cluster ions ($m = 10$) might be possible to exist, instead of the former. In the latter case, the molar ratio *M*/*W* would be 0.43, although main cluster ions are completely the same for both cases. According to the vapor–liquid equilibrium data, the mole fraction of methanol in the vapor phase

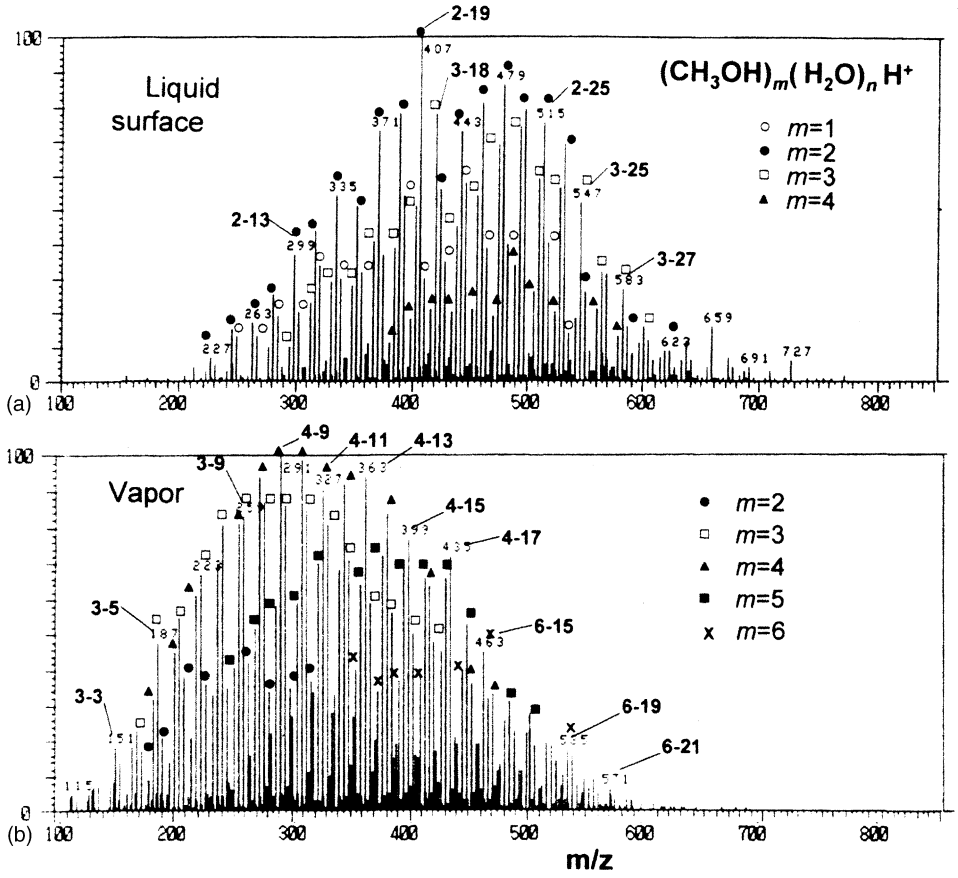

Fig. 3. LPI mass spectra of 20% (v/v) methanol aqueous solution: (a) measured at the liquid surface using the device B (sample flow rate: 0.5 μl/min) and (b) measured in the gas phase using the device C (sample flow rate: 0.3 μl/min).

for 20% methanol solution has been reported as 0.47 ($M/W = 0.88$) [27]. It seems reasonable to consider that the results shown in Tables 5 and 6 present the cluster composition distributions in the gas phase near the liquid surface, although the sizes of observed cluster ions are larger than expected.

3.3. Size and abundance distributions of cluster ions

The correlations between the relative abundances of cluster ions and the number of molecules, *m* and *n*, are presented in Figs. 4 and 5, respectively. The abscissa of Fig. 4 indicates the number of ethanol molecules (*m*) in each cluster ion and the ordinate indicates the relative abundance of the sum of cluster ions containing *m* molecules of ethanol. Similarly in Fig. 5, the abscissa indicates the number of water molecules (*n*) in each cluster ion and the ordinate indicates the relative abundance of the sum of cluster ions containing *n* molecules of water. Relative abundance was calculated from the sum of peak intensities for all cluster ions containing the same number of ethanol molecules ($\sum Im$) or of water molecules ($\sum In$), respect to the total ions (the sum of peak intensities for all cluster ions in a mass spectrum). That is $\sum Im/\sum(\sum Im)$ in Fig. 4 and $\sum In/\sum(\sum In)$ in Fig. 5. $\sum(\sum Im) = \sum(\sum In)$.

As previously described, Fig. 4 indicates clearly that the cluster ions containing two molecules of ethanol are the most abundant for the 20% ethanol solution and the numbers of ethanol molecules in clusters increased gradually to three and four during evaporation. The difference between the liquid surface (close to the bulk) and in the gas phase (3 mm above the liquid surface) is relatively small. In contrast, Fig. 5 indicates that the numbers of water molecules in clusters decreased sharply during evaporation. The reproducibility of the number distribution of water molecules in the gas phase was good, being almost independent from the sample flow rate between 0.3 and 0.6 μl/min. The results clearly indicate that the main processes occurred during evaporation is the elimination of water molecules (and clusters) from each clusters at the liquid surface. When using wider surface area (diameter: 2 mm), residual water clusters at the liquid surface have been observed sometimes [25].

The abscissa of Fig. 6 indicates the number of methanol molecules (*m*) and the ordinate indicates the relative abundance of all cluster ions containing *m* molecules of methanol. Fig. 7 indicates the same as those in Fig. 5 for the methanol aqueous solution.

Results indicate that for both alcohol solutions main process in the initial stage of evaporation is the dissociation

Table 4
Digital expression of the mass spectrum (Fig. 3a) of 20% methanol solution measured with device B; peak intensity > 410 = R.I. > 1.5%, > 140 = R.I. > 0.5%, R.I.: relative ion abundance = *Im* − *n*/total ions

n \ *m*	M0	M1	M2	M3	M4	M5	M6	M7	Σ*In*	*n*Σ*In*
0										
1										
2										
3										
4										
5										
6										
7				33					33	231
8				34					34	272
9			72						72	648
10		39	144	97	37				317	3170
11		50	160	98	59				367	4037
12		122	**234**	**208**	64	62			690	8280
13		125	**334**	**268**	103				830	10790
14		**180**	**401**	**256**	106	47			990	13860
15		**187**	493	**377**	**164**	45			1266	18990
16	38	**311**	466	**357**	**197**	44			1413	22608
17	43	**273**	662	468	**186**				1632	27744
18	29	**291**	704	**711**	**196**	48	47		2026	36468
19	72	**341**	**902**	408	**175**	79	29	37	2043	38817
20	81	**490**	514	492	**307**			32	1916	38320
21	49	**275**	661	630	**240**	58			1913	40173
22	42	**321**	737	669	**186**				1955	43010
23	76	525	779	540	**163**	36		28	2147	49381
24	64	**354**	715	513	**197**				1843	44232
25	48	**364**	681	**471**	121				1685	42125
26	88	**379**	**630**	**291**	103				1491	38766
27		**362**	**241**	**249**	72				924	24948
28	66	132	**280**	**151**	61				690	19320
29	52	87	**146**	82					367	10643
30		32	115	103					250	7500
31	31	81	86	39	31				268	8308
32		62	60	37					159	5088
33		37	150	43					230	7590
34			37	28					65	2210
35				59					59	2065
Σ*Im*	779	5420	10404	7712	2768	419	76	97	27675	
*m*Σ*Im*		5420	20808	23136	11072	2095	456	679		569594
								63666	*M/W*=0.112	

Table 5
Digital expression of the mass spectrum (Fig. 3b) of the 20% methanol solution measured with device C; peak intensity > 1410 = R.I. > 1.5%, > 470 = R.I. > 0.5%

n \ *m*	M0	M1	M2	M3	M4	M5	M6	M7	M8	M9	Σ*In*	*n*Σ*In*
0					**102**	**111**					213	
1				101	140	179					420	**420**
2				145	361	283	109		89	65	1052	**2104**
3			69	361	**639**	432	177	143		75	1896	**5688**
4			139	**473**	**898**	**655**	320	143			2628	**10512**
5			283	**951**	**1217**	**816**	441	218	90	81	4097	**20485**
6			347	**1106**	**1400**	**1043**	**536**	202	76	101	4811	**28866**
7			428	**1330**	1621	**1158**	**681**	266	116	66	5666	**39662**
8			**770**	1621	1880	**1170**	**662**	219	151		6473	**51784**
9		100	**725**	1645	**1981**	**1392**	**810**	306	109		7068	**63612**
10		82	**699**	1740	1974	**1350**	**692**	322	126	67	7052	**70520**
11		98	**842**	1704	1816	**1283**	**741**	348	107		6939	**76329**
12		128	**684**	1691	1829	**1442**	**765**	387	139	61	7126	**85512**
13		68	**705**	1617	1875	**1374**	**910**	384	78		7011	**91143**
14		92	**737**	1426	1669	**1325**	**800**	263			6312	**88368**
15		76	**573**	**1184**	1532	**1322**	**904**	227	69		5887	**88305**
16		78	**544**	**1118**	**1272**	**1065**	**530**	151			4758	**76128**
17			414	**999**	**1444**	**641**	436	211			4145	**70465**
18		105	382	**959**	**722**	**621**	390	184			3363	**60534**
19			309	433	**660**	**545**	344				2291	**43529**
20		78	177	394	468	361	131	61			1670	**33400**
21			110	218	369	298	137				1132	**23772**
22			133	244	282	196	76				931	**20482**
23		77		131	140	79					427	**9821**
24				142	113						255	**6120**
25				102							102	**2550**
26			64								64	**1664**
Σ*Im*	0	982	9134	21835	26404	19141	10592	4035	1150	516	93789	
m*Σ*Im		**982**	**18268**	**65505**	**105616**	**95705**	**63552**	**28245**	**9200**	**4644**	**W=1071775**	
										391717	***M/W*=0.365**	

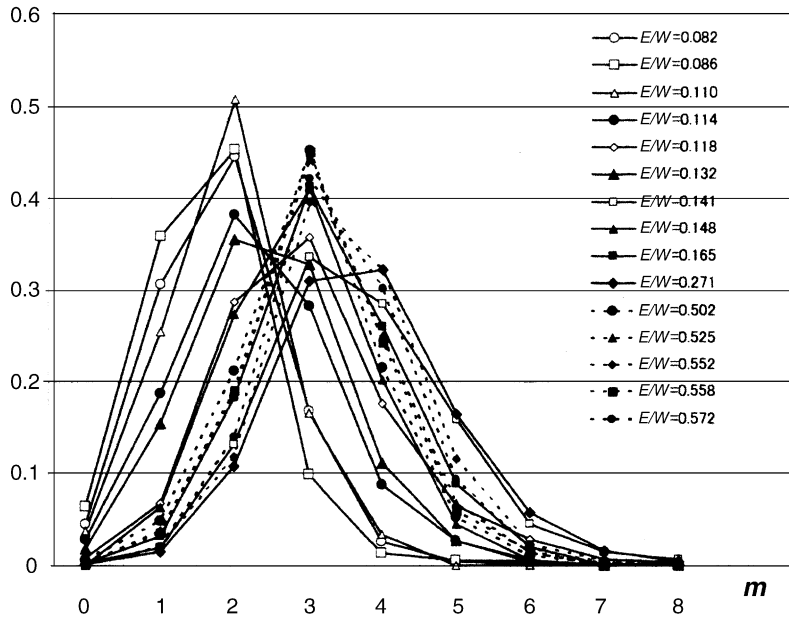

Fig. 4. Distribution of the relative abundances of cluster ions containing *m* molecules of ethanol as a function of the number of ethanol molecules (*m*) for the 20% ethanol solution. Relative abundance: the sum of peak intensities of al! ions containing *m* molecules of ethanol, respect to the total ions (1.00) in each mass spectrum, (—●—) measured with the device A, (—○—) measured with the device B, and (- - ● - -) measured with the device C.

Table 6
Digital expression of LPI mass spectrum of the 20% methanol solution measured with device C; peak intensity > 4600 = R.I. > 1.5%, > 1540 = R.I. > 0.5%

n \ *m*	M0	M1	M2	M3	M4	M5	M6	M7	M8	M9	*ΣIn*	*nΣIn*
0												
1									226	247	473	**473**
2						183	307	318	272	283	1363	**2726**
3						397	545	549	416	273	2180	**6540**
4					338	782	1041	856	517	435	3969	**15876**
5					614	1366	1456	1055	681	603	5775	**28875**
6				309	1082	**2023**	**1916**	1507	856	862	8555	**51330**
7				661	**1829**	**2401**	2299	**1854**	1334	848	11226	**78582**
8				889	**2321**	**3306**	**2841**	**2158**	**1571**	910	13996	**111968**
9			214	1199	**2971**	**4066**	**3510**	**2631**	**1708**	1001	17300	**155700**
10			324	1527	**3219**	**4215**	**4305**	**3059**	**1916**	1158	19723	**197230**
11			524	**1766**	**3689**	4735	4781	**3198**	**2216**	1277	22186	**244046**
12			535	**2008**	**3940**	5274	4761	**3581**	**2352**	1330	23781	**285372**
13		173	617	**2030**	**4171**	5305	5295	**3700**	**2633**	1313	25237	**328081**
14			624	**2144**	**4115**	**5542**	5273	**4112**	**2095**	971	24876	**348264**
15			574	**2010**	**4248**	5458	**5471**	**3414**	**1694**	894	23763	**356445**
16			581	**2005**	**3724**	**5416**	**3630**	**2616**	**1626**	833	20431	**326896**
17			706	**1756**	**3914**	**3526**	**3141**	**2506**	**1722**	571	17842	**303314**
18		312	674	**1763**	**2318**	**3009**	**2879**	**2300**	800		14055	**252990**
19		307	652	1102	**2120**	**2908**	**2450**	844	882		11265	**214035**
20		333	496	1038	**1799**	**2274**	**1669**	1211	643		9463	**189260**
21		463	480	970	**1614**	**1576**	771	988	393		7255	**152355**
22		515	540	882	1054	1300	1219	549	280		6339	**139458**
23		642	483	613	861	901	593	430			4523	**104029**
24		658	379	439	573	689	422	205			3365	**80760**
25		503	372	391	243	424					1933	**48325**
26		678	361	186	227	201	180				1833	**47658**
27		673	360		245	174					1452	**39204**
28		508	204	201							913	**25564**
29		488	189								677	**19633**
30		210									210	**6300**
31		426									426	**13206**
32		174									174	**5568**
33		187									187	**6171**
ΣIm		**7250**	**9889**	25889	51229	67451	60755	43641	26833	13809	306746	
mΣIm		**7250**	**19778**	**77667**	**204916**	**337255**	**364530**	**305487**	**214664**	**124281**		**W=4186234**
									M=1655828			***M/W*=0.396**

of clusters through loss of water molecules. In the case of methanol solution, the increase in the number of methanol molecules occurred more significantly than in the case of ethanol solution, probably because methanol and water molecules dissolve more freely than ethanol and the following collisions between smaller clusters may lead to the association of smaller clusters accompanied with the loss of water, resulting in the increase in the number of methanol molecules in clusters. In contrast, the main processes for the ethanol solution are the loss of water, probably because ethyl is more hydrophobic than methyl. It is interesting to note that in the following processes, the association occurred mainly between ethanol molecules with continuous loss of water molecules, resulting in the formation of ethanol clusters $(C_2H_5OH)_m$ ($m = 2$–6 in Table 3), while almost no methanol clusters were observed (Tables 5 and 6).

The *E*/*W* ratios measured with the device A were higher than that of the concentration. The reason for this was thought to be that the thickness of liquid layer at the needle tip was thinner in the device A compared with the device B and thus, the evaporation of liquid occurred more rapidly to give higher ethanol concentration. The new device B

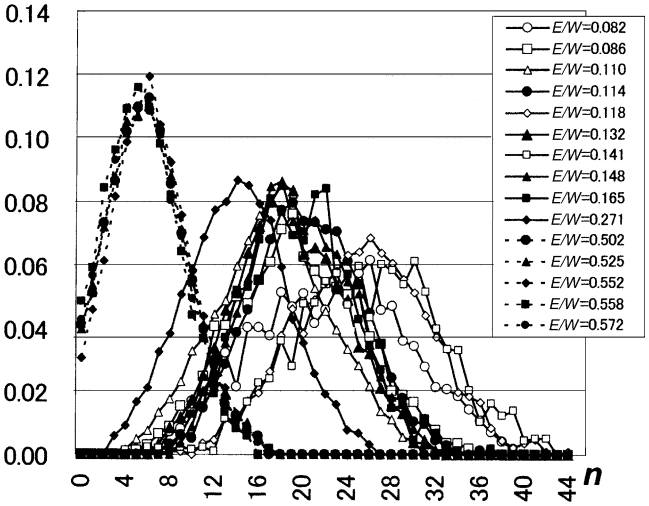

Fig. 5. Distribution of the relative abundances of cluster ions containing *n* molecules of water as a function of the number of water molecules (*n*) for the 20% ethanol solution. Relative abundance: the sum of peak intensities of all ions containing *n* molecules of water/total ions (1.00) in each mass spectrum. (—●—) measured with the device A, (—○—) measured with the device B, and (- -●- -) measured with the device C.

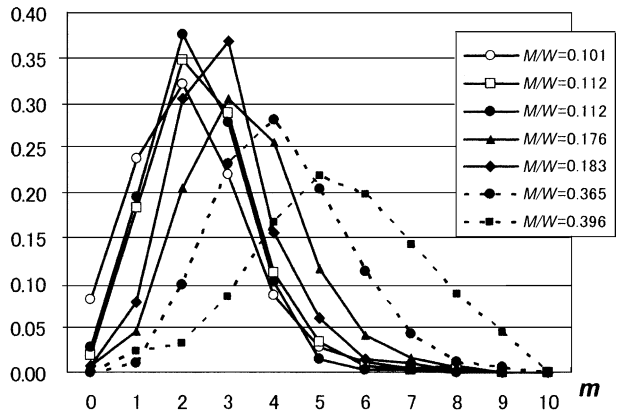

Fig. 6. Distribution of the relative abundances of cluster ions containing *m* molecules of methanol as a function of the number of methanol molecules (*m*) for the 20% methanol solution. Relative abundance: the sum of peak intensities of all ions containing *m* molecules of methanol/total ions (1.00) in each mass spectrum. (—●—) measured with the device A, (—○—) measured with the device B, and (- - ● - -) measured with the device C.

provided better results with smaller *m*, larger *n* and the molar ratios close to the concentration. The results suggest that ideal conditions for measuring liquids should be ionizing whole sample at the liquid surface prior to evaporation.

3.4. Structure of clusters

The cluster ion containing 21 molecules of water ($m = 21$) has been well known as magic number cluster [1,2] and such magic number clusters have been also observed in binary systems ($m + n = 21$) [11,12]. LPI mass spectra also showed such magic number cluster ions both for the ethanol and methanol solutions as seen in Tables 1, 2, 4-6 and Figs. 2a, 3a and b, in which the intense peaks such as 1–20, 2–19, 3–18, 4–17, 5–16 and 6–15 are observed. In addition, the cluster ions of 3–18 and 4–17 have been

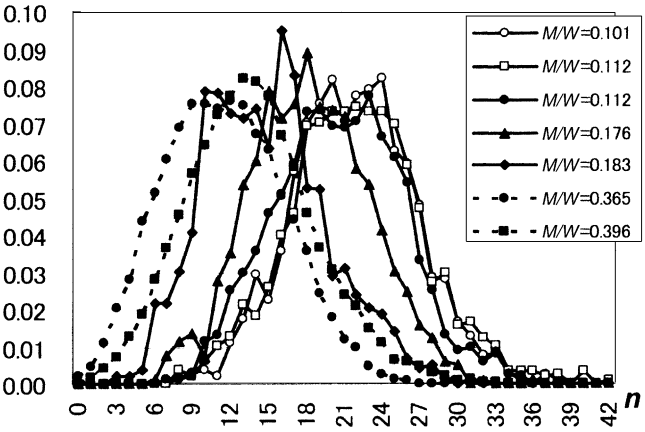

Fig. 7. Distribution of the relative abundances of cluster ions containing *n* molecules of water as a function of the number of water molecules (*n*) for the 20% methanol solution. Relative abundance: the sum of peak intensities of ail ions containing *n* molecules of water/total ions (1.00) in each mass spectrum.

the most abundant ions for 40% ethanol aqueous solutions [25]. Additionally, another magic number (28) of water is also observed in Fig. 2a (base peak: 2–26) and weakly in Table 4 (1–27, 2–26, 3–25 and 4–24). The results suggest that the structures of water clusters are kept in both solutions and water molecules in the clusters are replaced by alcohol molecules one by one, in early stage of reactions.

The cluster ions of 2–19 are often abundant for 20% solutions, because they may have similar structure to the magic number cluster ($n = 21$) of water. Pentagonal dodecahedron has been suggested as the structure of the magic number (21) cluster of water [2]. The existence of abundant cluster ions with smaller sizes ($m + n < 21$), however, suggests that most of the clusters in the liquids may be constructed of networks of five-membered rings and six-membered rings.

4. Conclusion

The composition distribution of neutral clusters in the solution may be under a sort of semi-equilibrium state, which depends on the temperature and alcohol concentration of the solution. The cluster (neutral) compositions, however, vary very quickly (in the order of pico-seconds), especially at the liquid surface, because the density of liquid is 1000 times higher than that in a gas phase and it has been also well known for methanol–water and ethanol–water mixtures that the mole fraction of alcohol in vapor is much higher than that in the liquid [14].

The averaged molar ratios (*E*/*W* and *M*/*W*) calculated from the mass spectra measured with the device B gave the values close to the ratios corresponding to the concentrations of the solutions. Furthermore, the abundant cluster ions were observed around the base peak and the molar ratios calculated from the compositions (*m*/*n*) of abundant cluster ions agreed with that of the averaged molar ratio calculated from whole mass spectrum, even in the gas phase (Tables 3, 5 and 6). Agreement between the observed ratios and the expected ratios suggest that the observed cluster ions might be similar to the clusters existing at the liquid surface.

It is certain that the cluster ions are produced in the LPI ion source under atmospheric pressure at ambient temperature. All results indicate that the adiabatic condensation can be neglected and the cluster ions are rather stable, being observed without dissociation during flight from the ion source to the collector. The results shown in all tables suggest that the efficiencies of ionization and detection for various clusters in the samples may be nearly the same and mass spectra are likely to present the size distribution of neutral clusters at and above the liquid surface.

It is likely that the number of alcohol molecules in clusters seems to be one of the most important parameters for estimating the cluster compositions in liquids, because these numbers are related to the concentration of the solutions. It is assumed that the liquid might be an aggregate of groups

of clusters similar to those observed as the LPI mass spectra (as shown in Tables 1, 2 and 4).

The evaporation processes occurring in the nano-space at and above the liquid surface are mainly the loss of water molecules from larger clusters. The following collisions between smaller clusters lead to the association of alcohol molecules accompanied with further loss of water molecules. The increase in the number of methanol molecules was more significant than the case of ethanol–water, probably because methanol and water molecules dissolve more freely and combine more strongly than ethanol and water. The significant loss of water with slight increase in the number of ethanol molecules may be reasonable for the ethanol solution, because ethyl is more hydrophobic than methyl.

In previous methods utilizing adiabatic expansion, abundant ethanol cluster ions accompanied by small numbers of large binary cluster ions have been observed for ethanol–water mixtures [9]. It is assumed that the decomposition of binary clusters occurs instantaneously to produce abundant ethanol molecules when the sample enter into the vacuum, and the adiabatic condensation produce abundant ethanol clusters and small numbers of large binary clusters in the center of the molecular beam.

LPI mass spectrometry is useful for investigating hydrogen-bonded clusters at and above the liquid surface, the evaporation processes and the structure of clusters in liquids.

References

[1] J.Q. Searcy, J.B. Fenn, J. Chem. Phys. 61 (1974) 5282.
[2] P.M. Holland, A.W. Castleman Jr., J. Chem. Phys. 72 (1980) 5984.
[3] V. Hermann, B.D. Kay, A.W. Castleman Jr., Chem. Phys. 72 (1982) 185.
[4] R.J. Beuhler, L. Friedman, J. Chem. Phys. 77 (1982) 2549.
[5] A.W. Castleman Jr., R.G. Keesee, Chem. Rev. 86 (1986) 589.
[6] J.F. Garvey, W.J. Herron, G. Vaidyanathan, Chem. Phys. 94 (1994) 1999.
[7] K. Liu, J.D. Cruzan, R.J. Saykally, Science 271 (1996) 929.
[8] N. Nishi, K. Yamamoto, J. Am. Chem. Soc. 109 (1987) 7353.
[9] N. Nishi, K. Koga, C. Ohshima, K. Yamamoto, U. Nagashima, K. Nagami, J. Am. Chem. Soc. 110 (1988) 5246.
[10] T. Ebata, A. Fujii, N. Mikami, Int. Rev. Phys. Chem. 17 (1998) 331.
[11] Z. Shi, S. Wei, J.V. Ford, A.W. Castleman Jr., Chem. Phys. Lett. 92 (1992) 142.
[12] A. Wakisaka, H. Abdoul-Carime, Y. Yamamoto, Y. Kiyozumi, J. Chem. Soc., Faraday Trans. 94 (1998) 369.
[13] G. Raina, G.U. Kulkarni, C.N.R. Rao, Int. J. Mass Spectrom. 212 (2001) 267.
[14] R.C. Pemberton, C.J. Mash, J. Chem. Thermodyn. 10 (1978) 867.
[15] M. Tsuchiya, H. Kuwabara, Anal. Chem. 56 (1984) 14.
[16] M. Tsuchiya, Advances in Mass Spectrometry, vol. 13, John Wiley, New York, 1995, p. 333.
[17] M. Tsuchiya, Mass Spectrom. Rev. 17 (1998) 51.
[18] M. Tsuchiya, E. Aoki, H. Kuwabara, Int. J. Mass Spectrom. Ion Processes 90 (1989) 55.
[19] Y. Li, T. Tashiro, K. Hama, M. Tsuchiya, in: Proceedings of the ASMS Conference, Portland, Oregon, May 1996, p.76.
[20] M. Tsuchiya, T. Tashiro, A. Shigihara, J. Mass Spectrom. Soc. Jpn. 52 (2004) 1.
[21] M. Tsuchiya, S. Teshima, T. Kaneko, T. Hirano, Nippon Kagaku Kaishi (1993) 687.
[22] M. Tsuchiya, Y. Li, J. Shirasaka, T. Kaneko, Chem. Lett. (1996) 229.
[23] Y. Li, J. Shirasaka, M. Kouzaki, T. Kaneko, M. Tsuchiya, J. Mass Spectrom. Soc. Jpn. 45 (1997) 459.
[24] M. Tsuchiya, M. Tajima, Y. Shida, K. Kobayashi, S. Okouchi, Anal. Sci. 17 (Suppl.) (2001) i95.
[25] M. Tsuchiya, Y. Shida, K. Kobayashi, M. Tajima, S. Okouchi, Bunseki Kagaku 51 (2002) 943.
[26] S. Tomoda, K. Kimura, Chem. Phys. Lett. (1983) 560.
[27] M.L. McGlashan, J. Chem. Eng. Data 21 (1976) 196.